

Calcareous Nannofossil Biostratigraphy and Stage Boundaries of the Santonian-Eocene Successions in Wadi El Mizeira Northeastern Sinai, Egypt

Hamza Khalil¹, Esam Zahran²

¹Geology Department, Faculty of Science, Tanta University, Tanta, Egypt

²Geology Department, Faculty of Science, Damanhour University, Damanhour, Egypt

Email: hamzakhali2002@yahoo.com

Received 13 February 2014; revised 15 March 2014; accepted 11 April 2014

Copyright © 2014 by authors and Scientific Research Publishing Inc.

This work is licensed under the Creative Commons Attribution International License (CC BY).

<http://creativecommons.org/licenses/by/4.0/>



Open Access

Abstract

The stratigraphic successions exposed in Wadi El Mizeira have been dated through the analysis of the calcareous nannofossil assemblages. The results of this study indicate that the successions comprise the Santonian-Late Maastrichtian (Sudr Formation), the Paleocene (Esna Formation) and the Early Eocene (Thebes Formation). The following biozones were recognized: Late Santonian, CC16 Zone; Late Santonian/Early Campanian, CC17 Zone; Early Campanian, *Aspidolithus parvus* Zone (CC18) Zone; Late Maastrichtian, CC25c Zone; Early Paleocene (Late Danian), NP3 Zone and NP4 Zone; Late Paleocene (Thanethian-Selandian), NP5 Zone; Early Eocene, NP9b Zone, NP10a Zone, NP11 Zone, NP12 Zone and NP14 Zone. Several stratigraphic hiatus were recorded in the studied interval including the absence of Cretaceous nannofossil Zones CC19 to CC25b and CC26 as well as the early Paleocene Zones NP1 and NP2 and probably the basal part of Zone NP3, in addition to the absence of the Zones NP6 and NP7/8. These hiatus may be attributed to environmental conditions, structural activity and/or post depositional processes. This work represents the first attempt to evaluate the nannofossil taxa of the Wadi El Mizeira, Northeastern Sinai.

Keywords

Calcareous Nannofossil, Biostratigraphy, Santonian, Eocene, Sinai, Egypt

1. Introduction

The Upper Cretaceous-Lower Paleogene sediments are well developed in the stratigraphic successions of Sinai.

How to cite this paper: Khalil, H. and Zahran, E. (2014) Calcareous Nannofossil Biostratigraphy and Stage Boundaries of the Santonian-Eocene Successions in Wadi El Mizeira Northeastern Sinai, Egypt. *International Journal of Geosciences*, 5, 432-449. <http://dx.doi.org/10.4236/ijg.2014.54041>

A relatively thick Santonian-Eocene sequence was measured and sampled from Wadi El Mizeira, Northeastern Sinai (**Figure 1**). Wadi El Mizeira (about 35 km south of El Qussaima) extends to the north and west around Gabal Araif El-Naqa. The Upper Cretaceous Sudr Chalk is exposed forming the floor of the wadi and the foot-slope of Senaf El Mizeira ridge, while, the Thebes Formation forming the prominent cliff of Senaf El Mizeira Ridge.

The paleontological aspects of the Upper Cretaceous-Lower Paleogene in north east Sinai have been the subject of several studies [1]-[31] because of its relative richness in microfossils and expanded stratigraphic records. The published data on the calcareous nannofossil biostratigraphy in northeastern Sinai are scarce. The purpose of the present study is to establish a calcareous nannofossil biostratigraphic framework and define the stage boundaries and biostratigraphic hiatus for the Santonian-Early Eocene sediments at Wadi El Mizeira.

2. Material and Methods

Calcareous nannofossil analyses have been performed for 129 samples taken on average every 1 m; with high resolution sampling adopted close to key biohorizons. Calcareous nannofossils are generally abundant and well diversified in the studied sequence, with a good degree of preservation.

Samples were processed by smear slide preparation from raw sediment samples [32]. All samples were prepared similarly to insure uniformity in the distribution and to minimize bias. Relative species abundances were determined by counting a population of at least 300 specimens along a random traverse with a light microscope at a magnification of about 1250 \times . Rare species were searched in two additional traverses across the slide to assure that no stratigraphic marker was overlooked. Total nannofossil abundance was calculated as the total number of specimens counted per number of fields of view (FOV) traversed.

Preservation was estimated as Good (G) for nannofossil specimens exhibiting little or no dissolution; Moderate (M) for moderate dissolution and/or overgrowth and Poor (P) for strong dissolution and/or over growth. A fully referenced taxonomic listing appears in [33]. The stratigraphic distribution, preservation and abundance of the nannofossils are provided in a distribution charts (**Figures 3-5**).

3. Lithostratigraphy

The Santonian-Eocene succession exposed at Wadi Mizeira is generally composed of carbonate sediments. Lithostratigraphically, the succession is subdivided from base to top into; the Sudr, the Esna and the Thebes Formations (**Figure 2**).

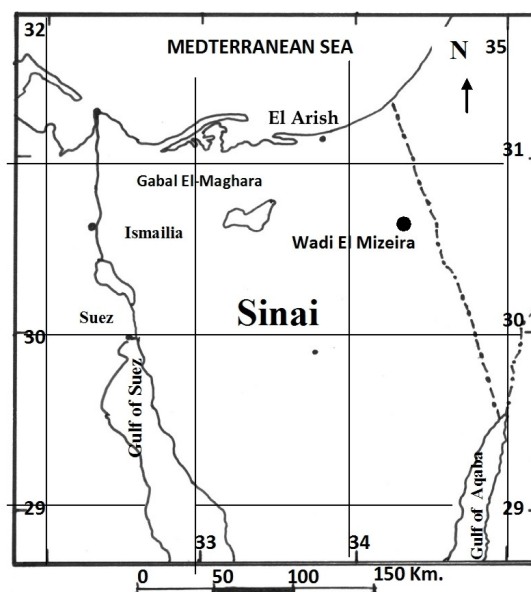


Figure 1. Location map of Wadi El Mizeira, Northeastern Sinai.

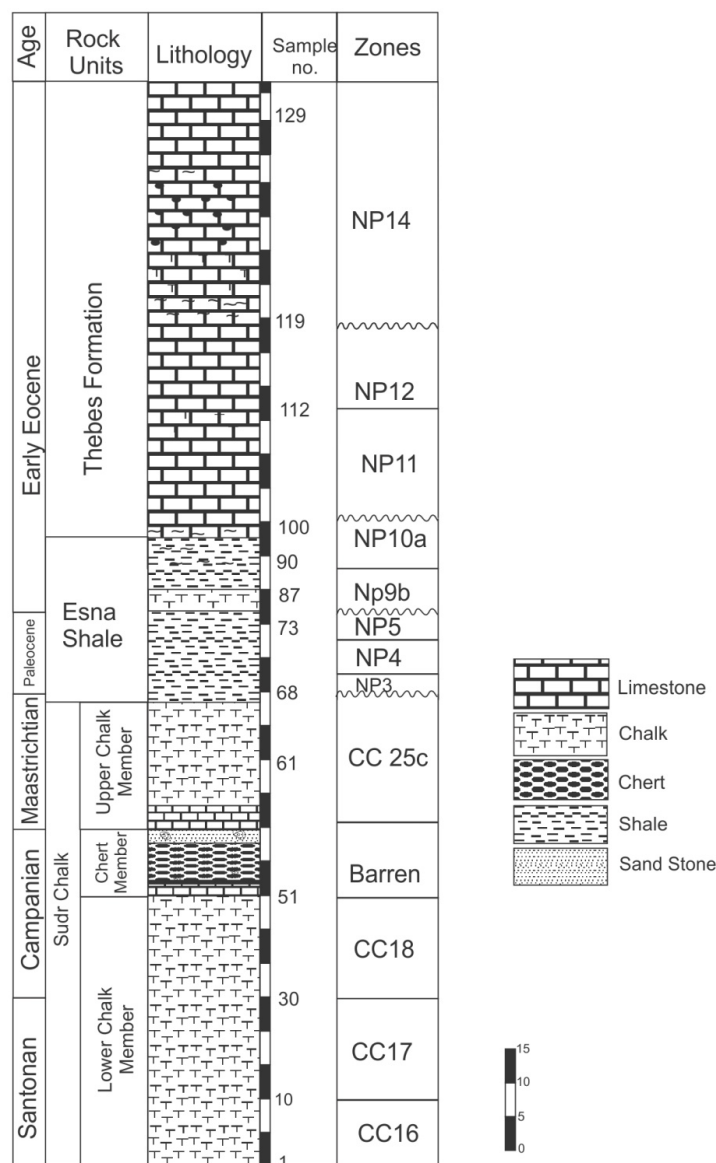


Figure 2. Litho- and calcareous nannofossil biostratigraphy of the Santonian-Eocene succession in Wadi El Mizeira, Sinai.

3.1. Sudr Formation

The term Sudr Chalk was originally introduced by [34] for the chalky limestone succession exposed at Wadi Sudr, west central Sinai. In the present study the Sudr Formation is exposed along the floor of Wadi El Mizeira and the foot-slope of Senaf El Mizeira Ridge. It is predominantly composed of chalk, chalky limestone with shale intercalations, siliceous limestone, chert and bioclastics. The Sudr Chalk could be subdivided into; the Lower Chalk Member, the Chert Member and the Upper Chalk Member.

The Lower Chalk Member attains a thickness of about 35 m and consists mainly of hemipelagic soft snow-white massive chalk. The middle Chert Member exhibits distinctive lithologic characters and is composed of dark chert, siliceous limestone, siliceous sandstone and bioclasts. It attains about 10 m thick and contains few phosphatic beds and oyster banks. The Upper Chalk Member (about 18 m thick) is composed of chalk and chalky limestone grads into argillaceous chalk at the top. The calcareous nannofossil content assigned the Lower Chalk Member to Santonian-Early Campanian age and the Upper Chalk Member to Late Maastrichtian age. The stratigraphic position of the Middle Chert Member points to Late Campanian - Early Maastrichtian age.

Upper Cretaceous										Age	
Santonian					Campanian					Late Maastrichtian	
Sudr Chalk										Rock units	
Lower Chalk Member										Upper Chalk Member	
CC16										CC25c	
CC17										CC18	
CC18										CC25c	
CC19										CC20	
CC21										CC22	
CC23										CC24	
CC25										CC26	
CC27										CC28	
CC29										CC30	
CC31										CC32	
CC33										CC34	
CC35										CC36	
CC37										CC38	
CC39										CC40	
CC41										CC42	
CC43										CC44	
CC45										CC46	
CC47										CC48	
CC49										CC50	
CC51										CC52	
CC53										CC54	
CC55										CC56	
CC57										CC58	
CC59										CC60	
CC61										CC62	
CC63										CC64	
CC65										CC66	
CC67										CC68	
CC69										CC70	
CC71										CC72	
CC73										CC74	
CC75										CC76	
CC77										CC78	
CC79										CC80	
CC81										CC82	
CC83										CC84	
CC85										CC86	
CC87										CC88	
CC89										CC90	
CC91										CC92	
CC93										CC94	
CC95										CC96	
CC97										CC98	
CC99										CC100	
CC101										CC102	
CC103										CC104	
CC105										CC106	
CC107										CC108	
CC109										CC110	
CC111										CC112	
CC113										CC114	
CC115										CC116	
CC117										CC118	
CC119										CC120	
CC121										CC122	
CC123										CC124	
CC125										CC126	
CC127										CC128	
CC129										CC130	
CC131										CC132	
CC133										CC134	
CC135										CC136	
CC137										CC138	
CC139										CC140	
CC141										CC142	
CC143										CC144	
CC145										CC146	
CC147										CC148	
CC149										CC150	
CC151										CC152	
CC153										CC154	
CC155										CC156	
CC157										CC158	
CC159										CC160	
CC161										CC162	
CC163										CC164	
CC165										CC166	
CC167										CC168	
CC169										CC170	
CC171										CC172	
CC173										CC174	
CC175										CC176	
CC177										CC178	
CC179										CC180	
CC181										CC182	
CC183										CC184	
CC185										CC186	
CC187										CC188	
CC189										CC190	
CC191										CC192	
CC193										CC194	
CC195										CC196	
CC197										CC198	
CC199										CC200	
CC201										CC202	
CC203										CC204	
CC205										CC206	
CC207										CC208	
CC209										CC210	
CC211										CC212	
CC213										CC214	
CC215										CC216	
CC217										CC218	
CC219										CC220	
CC221										CC222	
CC223										CC224	
CC225										CC226	
CC227										CC228	
CC229										CC230	
CC231										CC232	
CC233										CC234	
CC235										CC236	
CC237										CC238	
CC239										CC240	
CC241										CC242	
CC243										CC244	
CC245										CC246	
CC247										CC248	
CC249										CC250	
CC251										CC252	
CC253										CC254	
CC255										CC256	
CC257										CC258	
CC259										CC260	
CC261										CC262	
CC263										CC264	
CC265										CC266	
CC267										CC268	
CC269										CC270	
CC271										CC272	
CC273										CC274	
CC275										CC276	
CC277										CC278	
CC279										CC280	
CC281										CC282	
CC283										CC284	
CC285										CC286	
CC287										CC288	
CC289										CC290	
CC291										CC292	
CC293										CC294	
CC295										CC296	
CC297										CC298	
CC299										CC300	
CC301										CC302	
CC303										CC304	
CC305										CC306	
CC307										CC308	
CC309										CC310	
CC311										CC312	
CC313										CC314	
CC315										CC316	
CC317										CC318	
CC319										CC320	
CC321										CC322	
CC323										CC324	
CC325										CC326	
CC327										CC328	
CC329										CC330	
CC331										CC332	
CC333										CC334	
CC335										CC336	
CC337										CC338	
CC339										CC340	
CC341										CC342	
CC343										CC344	
CC345										CC346	
CC347										CC348	
CC349										CC350	
CC351										CC352	
CC353										CC354	
CC355										CC356	
CC357										CC358	
CC359										CC360	
CC361										CC362	
CC363										CC364	
CC365										CC366	
CC367										CC368	
CC369										CC370	
CC371										CC372	
CC373										CC374	
CC375										CC376	
CC377										CC378	
CC379										CC380	
CC381										CC382	
CC383										CC384	
CC385										CC386	
CC387										CC388	
CC389										CC390	
CC391										CC392	
CC393										CC394	
CC395										CC396	
CC397										CC398	
CC399										CC400	
CC401										CC402	
CC403										CC404	
CC405										CC406	
CC407										CC408	
CC409										CC410	
CC411										CC412	
CC413										CC414	
CC415										CC416	
CC417										CC418	
CC419										CC420	
CC421										CC422	
CC423										CC424	
CC425										CC426	
CC427										CC428	
CC429										CC430	
CC431										CC432	
CC433										CC434	
CC435										CC436	
CC437										CC438	
CC439										CC440	
CC441										CC442	
CC443										CC444	
CC445										CC446	
CC447										CC448	
CC449										CC450	
CC451										CC452	
CC453										CC454	
CC455										CC456	
CC457										CC458	
CC459										CC460	
CC461										CC462	
CC463										CC464	
CC465										CC466	
CC467										CC468	
CC469										CC470	
CC471										CC472	
CC473										CC474	
CC475										CC476	
CC477										CC478	
CC479										CC480	
CC481										CC482	
CC483										CC484	
CC485										CC486	
CC487										CC488	
CC489										CC490	
CC491										CC492	
CC493										CC494	
CC495										CC496	
CC497										CC498	
CC499										CC500	
CC501										CC502	
CC503										CC504	
CC505										CC506	
CC507										CC508	
CC509										CC510	
CC511										CC512	
CC513										CC514	
CC515										CC516	
CC517										CC518	
CC519										CC520	
CC521										CC522	
CC523										CC524	
CC525										CC526	
CC527										CC528	
CC529										CC530	
CC531										CC532	
CC533										CC534	
CC535										CC536	
CC537										CC538	
CC539										CC540	
CC541										CC542	
CC543										CC544	
CC545										CC546	
CC547										CC548	
CC549										CC550	
CC551										CC552	
CC553										CC554	
CC555										CC556	
CC557										CC558	
CC559										CC560	
CC561										CC562	
CC563										CC564	
CC565										CC566	
CC567										CC568	
CC569										CC570	
CC571										CC572	
CC573										CC574	
CC575										CC576	
CC577										CC578	
CC579										CC580	
CC581										CC582	
CC583										CC584	
CC585										CC586	
CC587										CC588	
CC589										CC590	
CC591										CC592	
CC593										CC594	
CC595										CC596	
CC597										CC598	
CC599										CC600	
CC601										CC602	
CC603										CC604	
CC605										CC606	
CC607										CC608	
CC609										CC610	
CC611										CC612	
CC613										CC614	
CC615										CC616	
CC617										CC618	
CC619										CC620	
CC621										CC622	
CC623										CC624	
CC625										CC626	
CC627										CC628	
CC629										CC630	
CC631										CC632	
CC633										CC634	
CC635										CC636	
CC637										CC638	
CC639										CC640	
CC641										CC642	
CC643										CC644	
CC645										CC646	
CC647										CC648	
CC649										CC650	
CC651										CC652	
CC653										CC654	
CC655										CC656	
CC657										CC658	
CC659										CC660	
CC661										CC662	
CC663										CC664	
CC665										CC666	
CC667										CC668	
CC669										CC670	
CC671										CC672	
CC673										CC674	
CC675										CC676	
CC677										CC678	
CC679										CC680	
CC681										CC682	
CC683										CC684	
CC685										CC686	
CC687										CC688	
CC689										CC690	
CC691										CC692	
CC693										CC694	
CC695										CC696	
CC697										CC698	
CC699										CC700	
CC701										CC702	
CC703										CC704	
CC705										CC706	
CC707										CC708	
CC709										CC710	
CC711										CC712	
CC713										CC714	
CC715										CC716	
CC717										CC718	
CC719										CC720	
CC721										CC722	
CC723										CC724	
CC725										CC726	
CC727										CC728	
CC729										CC730	
CC731										CC732	
CC733										CC734	
CC735										CC736	
CC737										CC738	
CC739										CC740	
CC741										CC742	
CC743										CC744	
CC745										CC746	
CC747										CC748	
CC749										CC750	
CC751										CC752	
CC753										CC754	
CC755										CC756	
CC757										CC758	
CC759										CC760	
CC761										CC762	
CC763										CC764	
CC765										CC766	
CC767										CC768	
CC769										CC770	
CC771										CC772	
CC773										CC774	
CC775										CC776	
CC777										CC778	
CC779										CC780	
CC781										CC782	
CC783										CC784	
CC785										CC786	
CC787										CC788	
CC789										CC790	
CC791										CC792	
CC793										CC794	
CC795										CC796	
CC797										CC798	
CC799										CC800	
CC801										CC802	
CC803										CC804	
CC805										CC806	
CC807										CC808	
CC809										CC810	
CC811										CC812	
CC813										CC814	
CC815										CC816	
CC817										CC818	
CC819										CC820	
CC821										CC822	
CC823										CC824	
CC825										CC826	
CC827										CC828	
CC829										CC830	
CC831										CC832	
CC833										CC834	
CC835										CC836	
CC837										CC838	
CC839										CC840	
CC841										CC842	
CC843										CC844	
CC845										CC846	
CC847										CC848	
CC849										CC850	
CC851										CC852	
CC853										CC854	
CC855										CC856	
CC857										CC858	
CC859										CC860	
CC861										CC862	
CC863											

[illegible]

Figure 4. Distribution, abundance, preservation and biozones of the Paleocene-Eocene calcareous nannofossils in Wadi El Mizeira, Sinai.

3.2. Esna Shale

The term Esna Shale was first introduced by [35]. In the study area the Esna Formation (24 m thick) overlies the Upper Cretaceous Sudr Chalk and underlies the Lower Eocene Thebes Formation. At Wadi El Mizeira, the Esna Shale is predominantly composed of greenish gray shale, along Senaf El Mizeira Ridge the formation displays significant change in lithology and is made up of greenish hemipelagic marls, chalky with few grayish green shale intercalations in the middle part. The calcareous nannofossil content points to Late Maastrichtian to Early Eocene age for the Esna Shale.

3.3. Thebes Formation

The term Thebes Formation has been introduced by [36] to describe the limestone unit with chert bands overlying the Esna Shale in many parts of Egypt. At Wadi El Mizeira the Thebes Formation is well exposed forming the prominent cliff of Senaf El Mizeira Ridge. It is 65 m thick and composes of marls, marly chalk, and chalky limestone with chert bands and nodules. The formation exhibits lateral lithologic change and dominates with white chalk, siliceous limestone and some shale. The nannofossils content indicates an Early Eocene age for the Thebes Formation.

4. Biostratigraphy

In the present study, nannofossil biostratigraphic framework is applied according to the biozonation scheme of

[illegible]

Figure 5. Distribution, abundance, preservation and biozones of the Eocene calcareous nannofossils in Wadi El Mizeira, Sinai.

[37] [38] for the late Cretaceous and Early Eocene, respectively. A total of 109 nannofossil species were identified from the Upper Maastrichtian, Paleocene and Lower Eocene rocks of the studied section. Their stratigraphic distributions are shown on **Figures 3-5** and some representative calcareous nannofossil species are illustrated in **Plates 1-3**. Biostratigraphic subdivisions in the study area based on the calcareous nannofossils have been established and correlated with the standard biozones recognized in Egypt (**Table 1** and **Table 2**) and other parts of the world.

Twelve nannofossil zones are identified in the studied area (Santonian to Early Eocene), based on the first and last occurrences (FOs, LOs) of the marker species. The Upper Cretaceous rocks comprise CC16, CC17, CC18 and CC25c. The Lower Paleogene rocks comprise eight zones from NP3, NP4, NP5, NP9b, NP10a, NP11, NP12 and NP14. The recognized biozones and subzones and the correlation between them are discussed below.

5. Late Cretaceous Biozones

5.1. *Lucianorhabdus cayeuxii* Zone (CC16)

Definition: Interval from the FO of *L. cayeuxii* Deflandre to the FO of *Calculites obscurus* (Deflandre).

Author: [37].

Age: Late Santonian.

Thickness: 10 m; equivalent to the lower part of the Lower Chalk Member.

Table 1. Correlation of Santonian-Maastrichtian calcareous nannofossil biostratigraphy of Wadi El Mizeira section with other biostratigraphic schemes in Sinai and Western Desert.

Age	Biozones		[74] Western Desert	[28] East Central Sinai	[75] North East Sinai	[29] West Central Sinai	[76] West Central Sinai	Present Study	
Upper Cretaceous	Maastrichtian	CC26	Hiatus	CC26	CC26	Hiatus	Hiatus	CC26	Hiatus
		c						c	
		CC25	b	CC25	CC25	CC25		CC25	Hiatus
		a						Hiatus	
		CC24		CC24	Hiatus	CC24			
	CC23		CC23	CC23					
	CC22		CC22	CC22					
	Campanian	CC21		CC21	Hiatus	CC21		Hiatus	
		CC20		CC20		CC20			
		CC19		CC19		CC19			
		CC18		CC18		CC18			
	Santonian	CC17	Hiatus	CC17	Hiatus	CC17		CC17	
		CC16		CC16		CC16			

Table 2. Correlation of Paleocene-Eocene calcareous nannofossil biostratigraphy of Wadi El Mizeira section with other biostratigraphic schemes in Sinai.

Age	Biozones	[77] North Central Sinai	[75] North East Sinai	[78] West Central Sinai	[79] North Sinai	[80] North Central Sinai	Present Study
Eocene	NP14	Hiatus		Hiatus	Np14	Hiatus	NP14
	Np13				NP13		Hiatus
	NP12	Hiatus	NP12	Hiatus	NP12		
	NP11	NP11	NP11		NP11		
	NP10	NP10	Np10		NP10		
	b	Hiatus	Hiatus	Hiatus	Hiatus	b	
	NP9						NP9
a	a	a	Hiatus				Hiatus
Paleocene	NP7/8	NP7/8	NP7/8	NP7/8	Hiatus	Np7/8	Hiatus
	NP6	NP6	NP6	NP6		NP6	
	NP5	NP5	NP5	NP5		NP5	NP5
	NP4	NP4	NP4	NP4	NP4	NP4	NP4
	Np3	NP3	NP3	NP3	NP3	NP3	NP3
	NP2	NP2	NP2	NP2	NP2	Hiatus	Hiatus
	NP1	Hiatus	Hiatus	NP1	Hiatus		

Assemblage: In general, the identified taxa in this zone are rare, but diversity is relatively high. In addition to the nominate taxon, this interval includes *W. béarnaise* and *Q. Gartner* among many other species.

Remarks: The first occurrence of *L. cayeuxii* is a very reliable event. Zone CC16 is equivalent to the upper

part of Zone UC11 and the UC12-13 zones of [39].

5.2. *Calculites obscurus* Zone (CC17)

Definition: This zone covers the interval from the FO of *Calculites obscurus* to the FO of *Aspidolithus parvus*.

Author: [37].

Age: Late Santonian/Early Campanian.

Thickness: 10 m; equivalent to the middle part of the Lower Chalk Member.

Assemblage: The assemblage of this interval is similar to that of the underlying CC16 Zone, with the addition of rare occurrences of the nominate taxon.

Remarks: According to [39], the first occurrence of *Arkhangelskiella cymbiformis* defines the base of Sub-zone UC13a of Early Campanian age. In the present study, rare specimens of *A. cymbiformis* have been observed in the Late Santonian (CC17), indicating that the range of the *A. cymbiformis* extends down into the Santonian. The FO of *Aspidolithus parvus* is an event that has been used for zonation and coincides reasonably well with the Santonian/Campanian boundary.

5.3. *Aspidolithus parvus* Zone (CC18)

Definition: Interval from the FO of *Aspidolithus parvus* to the LO of *Marthasterites furactus*.

Author: [37].

Age: Early Campanian.

Thickness: 15 m; equivalent to the upper part of the Lower Chalk Member.

Assemblage: Similar to the nannofossil assemblage from the CC17 Zone, with the addition of the nominate taxon *Aspidolithus parvus*.

Remarks: The upper boundary of the CC18 not well defined due to the absence of *M. furactus*. The first occurrence of *B. parcaparca* is a reliable global stratigraphic datum. Numerous workers have indicated that this datum marks the base of the CC18 Zone and serves as an approximation to the Santonian/Campanian boundary [16] [39]–[46]. The current study maintains this approximation because it can be correlated globally at all palaeolatitudes and in all palaeobiogeographical provinces [39] [46].

5.4. *Micula murus* Zone (CC25c)

Definition: It is defined as the interval from the FO of *Micula murus* to the FO of *N. frequens*.

Authors: [47], emended [48].

Age: Late Maastrichtian.

Thickness: 18 m; equivalent to the upper part of the Lower Chalk Member and the lower most part of the Esna Formation.

Assemblage: Besides the marker species, this zone is dominated by *Micula decussata*, *Watznaueria barnesae*, *Thoracosphaera operculata*, *Prediscosphaera cretacea*, *Eiffellithus gorkae*, *Arkhangelskiella cymbiformis*, *Eiffellithus turrisieffellii* and *Cyclagelosphaera reinhardtii*.

Remarks: In this study, this zone is identified from the first occurrence (FO) of *Miculamurust* to the FO of *N. frequens*. This zone correlates with the lower part of the *Nephrolithus frequens* Zone [49] modified by [50]. The *M. murus* Zone is probably restricted to low latitudes [50]. The top of CC25c is not defined accurately due to the absence of *M. prinsii*.

6. Paleocene and Eocene Biozones

6.1. *Chiasmolithus danicus* Zone (NP3)

Definition: FO of *Chiasmolithus danicus* to FO of *Ellipsolithus macellus*.

Author: [51].

Age: Early Paleocene (Late Danian).

Thickness: 2 m; equivalent to the lower part of the Esna Formation.

Assemblage: It is dominated besides the marker species by *Ericsonia cava* and relatively rare to very rare

occurrences of *Cruciplacolithus primus*, *Coccolithus pelagicus* and *Thoracosphaera operculata*.

Remarks: The upper boundary is defined by the FO of *Ellipsolithus macellus*, which is easy to recognize in well preserved material. In poorly preserved assemblages and/or in high latitudes, this species is missing but the zonal boundary can be identified by substitute evidence such as the absence of species of *Neochiastozygus* (*N. saepes*, *N. perfectus*), *Chiasmolithus bidens* and *Prinsius martinii*, all forms which are used to subdivide the high latitude Danian sections. *Chiasmolithus danicus* Zone is correlated to CP2 of [52].

6.2. *Ellipsolithus macellus* Zone (NP4)

Definition: FO of *Ellipsolithus macellus* to FO of *Fasciculithus tympaniformis*.

Author: [51].

Age: Early Paleocene (Late Danian).

Thickness: 5 m; equivalent to the lower part of the Esna Formation.

Assemblage: The calcareous nannofossil assemblage's characteristic of this zone contains *Chiasmolithus danicus*, *Cruciplacolithus primus*. *Cr. tenuus*, *Placozygus sigmoides* and *Ellipsolithus* spp. are occurred rarely in this zone. The first representatives of *Fasciculithus* (*F. billii*, *F. ulii* and *F. janii*); *Sphenolithus* (*Sphenolithus primus*) were also observed in this zone.

Remarks: Instead of the FO of *E. macellus*, the FO of *E. distichus*, another species of *Ellipsolithus*, appearing slightly after *E. macellus* where the two are consistently found together, has been used as a marker by some authors. *Ellipsolithus* is present from the lowermost studied sample upwards, thus indicating the presence of NP4. *Ellipsolithus macellus* Zone is equivalent to Zone CP3 of [52].

6.3. *Fasciculithus tympaniformis* Zone (NP5)

Definition: FO of *Fasciculithus tympaniformis* to FO of *Heliolithus kleinpellii*.

Authors: [53].

Age: Late Paleocene (Thanetian, Selandian).

Thickness: 4 m; equivalent to the middle part of the Esna Formation.

Assemblage: Nannofossil assemblages are similar to those recorded in NP4 but are distinguished by the presence of *F. tympaniformis* and *F. bitectus*.

Remarks: The lower boundary of NP5 was discussed above. Several new species such as *Heliolithus* and *Bomolithus* evolved before the FO of *H. kleinpellii* [50] [54]. *H. kleinpellii* was chosen as a zonal marker due to its wide distribution and easy recognition. The base of this zone is only recognized in the studied sequence. It is equivalent to *Fasciculithus tympaniformis* Zone, CP4 of [52].

6.4. *Discoaster multiradiatus* Zone (NP9b)

Definition: FO of *Discoaster multiradiatus* to FO of *Tribrachiatus bramlettei* or *Discoaster diastypus*.

Authors: [55] emended [56] [47].

Age: Early Eocene (Ypresian).

Thickness: 6 m; equivalent to the upper part of the Esna Formation.

Assemblage: The calcareous nannofossil assemblages; *Ericsonia cava*, *Ericsonia subpertusa*, *Coccolithus pelagicus*, *Chiasmolithus danicus*, *Fasciculithus involutus* and *Sphenolithus primus* occurred frequent to rarely in this zone.

Remarks: The definition of the upper boundary of NP9 is different from that of CP8, while the definition of the base is the same. Within NP9 several species of *Rhomboaster* evolve and can be used for a very fine subdivision of this interval [50] [57]. Several *Discoaster* species have their FO in NP9. The FO of *Discoaster multiradiatus* defines the base of Zones NP9 of [56] and CP8 of [52]. The FO of *D. multiradiatus* is considered a good reliable Paleocene datum in the Atlantic, Pacific and Mediterranean sections (e.g., [50] [53] [55] [58]-[65]). It is correlated with *Discoaster multiradiatus* Zone, CP8 of [52].

6.5. *Tribrachiatus contortus* Zone (NP10a)

Definition: FO of *Tribrachiatus bramlettei* to LO of *Tribrachiatus contortus*.

Authors: [66] and [67].

Age: Early Eocene (Ypresian).

Thickness: 9 m; equivalent to the lower part of the Thebes Formation.

Assemblage: In addition to the nominate taxon, this interval includes *Chiasmolithus consuetus*, *Discoaster lenticularis*, *Sphenolithus primus*, *Coccolithus pelagicus* and *Zygodiscus bijugatus*.

Remarks: NP10a has not been found in several sequences where it might be expected to present, probably due to the absence of the genus *Tribrachiatus* in certain areas for ecological reasons. When present, however, it is very easy to recognize NP 10 by the presence of *T. bramlettei* and/or *T. contortus*. Detailed studies of *T. bramlettei*, *T. contortus* and *T. orthostylus* were published by [50] [68]. In overgrown material both species have a tendency to look like ordinary calcite rhombohedron. Many species continue from the Paleocene into the Eocene, including some species, the FO of which is used as zonal markers in the Paleocene, i.e. *Ellipsolithus macellus* and *Discoaster multiradiatus*. *Fasciculithus* is only found in the lowermost part of NP 10 according to [50] and it's LO is used by other authors to define the Paleocene/Eocene boundary in sections where *Tribrachiatus* is very rare. It is correlated with *Tribrachiatus contortus* Subzone, CP9a of [52].

[69] subdivided the NP10 Zone into four subzones: NP10a (biostratigraphic interval from FO of *T. bramlettei* to the FO of *T. digitalis*); NP10b (total range of *T. digitalis*); NP10c (from LO of *T. digitalis* to the FO of *T. contortus*) and NP10d (total range of *T. contortus*). None of these subdivisions can be differentiated in the current study. This may be attributed to large space of sampling and/or small hiatus.

6.6. *Discoaster binodosus* Zone (NP11)

Definition: LO of *Tribrachiatus contortus* to FO of *Discoaster lodoensis*.

Authors: [53].

Age: Early Eocene (Ypresian).

Thickness: 17 m; equivalent to the middle part of the Thebes Formation.

Assemblage: *Discoaster distinctus*, *Sphenolithus editus*, *S. radians* and *S. conspicus* appear within NP11.

Remarks: *Tribrachiatus orthostylus*, a species which evolved from *T. contortus* appears near the NP10/NP11 boundary and evolves from a form with a slight bifurcation at the end of three arms to a form with three simple arms [50] [68] within NP11.

The top of NP10 is generally defined by the LO of *Tribrachiatus contortus* [32] [50] [56]. Alternatively, the FO of *Tribrachiatus orthostylus* takes place shortly before the LO of *Tribrachiatus contortus* and can be used as an approximation of the NP10/NP11 boundary [32]. We have tentatively placed that boundary at the FO of *Tribrachiatus orthostylus* so that our Zone NP11 may be a bit more reduced in reality than it appears. In this context, *Sphenolithus radians* record its FO at the base of NP11. It is correlated with *Discoaster binodosus* subzone, CP9b of [52].

In the present study, other nannofossil species occur in Zone NP11, such as *Zygrhablithus bijugatus*, *Discoaster barbadiensis*, *Discoaster binodosus*, *C. pelagicus*, *E. cava*, and *Chiasmolithus solitus*.

In several sections in Egypt [70]-[72], the *T. orthostylus* sometimes co-occurs with *T. contortus* at the extreme top part of zone NP10 or appears directly above the last occurrence of the latter, i.e., at the very base of Zone NP11. *T. orthostylus* was originally described from the Lower Eocene rocks of California and Austria [73]. In Egypt this species is predominate and characterize the Lower Eocene sediments. The stratigraphic value and occurrence of *Tribrachiatus orthostylus* as a guide fossil have already been proved [50].

6.7. *Tribrachiatus orthostylus* Zone (NP 12)

Definition: FO of *Discoaster lodoensis* to LO of *Tribrachiatus orthostylus*.

Authors: [67] [73].

Age: Early Eocene (Ypresian).

Thickness: 12 m; equivalent to the middle part of the Thebes Formation.

Assemblage: The most dominant species in addition to the marker species are *Coccolithus pelagicus*, *S. moriformis*, *Ericsonia Formosa* and *T. orthostylus*.

Remarks: The overlap of *D. lodoensis* and *T. orthostylus* is easily recognized in well preserved assemblages or in assemblages affected by dissolution. It is more difficult to recognize in assemblages affected by heavy overgrowth, where *T. orthostylus* and *D. lodoensis* are difficult to identify. It is equivalent to *Tribrachiatus orthostylus* Zone, CP10 of [52].

6.8. *Discoaster subloadoensis* Zone (NP14)

Definition: FO of *Discoaster subloadoensis* to FO of *Nannotetrina fulgens*.

Authors: [66] [67].

Age: Early Eocene.

Thickness: 38 m; equivalent to the upper part of the Thebes Formation.

Assemblage: It is dominated besides the marker species by *Coccolithus pelagicus*, *Ericsonia Formosa* and *D. lodoensis*.

Remarks: *D. lodoensis* overlaps with *D. subloadoensis* in the lower part of the zone and the FO of *R. inflata* is used to subdivide the zone into subzones CP12a and CP12b. The top of the zone has sometimes been approximated by using the FO of any species of *Nannotetrina* instead of *N. fulgens*, which can be very rare in some sections where other species of *Nannotetrina* are found consistently to be present. In these cases, *R. inflata* has been found overlap with *Nannotetrina*, *Sphenolithus furcatolithoides* and *S. spiniger* appear in the upper part of NP14. It is equivalent to *Discoaster subloadoensis* Zone, CP12 of [52], with a different definition for the top of the zone, when the LO of *R. inflata* is used as a substitute marker.

7. Stage Boundaries

The boundaries between stages are delineated based on the calcareous nannofossil datum events as follow:

1) Santonian/Campanian boundary

In the present samples the Santonian-Campanian boundary is marked by the last occurrences of *Calculites obscures* and the first occurrences of *Aspidolithus parvus*.

2) Campanian/Maastrichtian boundary

The Campanian/Maastrichtian boundary is not clear due to the absence of nannofossil assemblages as a result of post depositional changes.

3) The Cretaceous/Paleogene (K/Pg) boundary

The Cretaceous/Tertiary boundary is marked by the absence of the Late Cretaceous nannofossil Zone; CC26, as well as the Early Paleocene nannofossil biozones, NP1 and NP2 and probably the lower part of NP3.

4) Selandian/Thanethian boundary

A major hiatus is suggested at the Selandian/Thanethian boundary as indicated by absence of the nannofossil biozones; NP6, NP7 and NP8. On the other hand, the latest Paleocene calcareous nannofossil subzone NP9a is missed.

5) Paleocene/Eocene boundary

The Paleocene/Eocene boundary in the studied area is correlative to the base of the *Discoaster multiradiatus* NP9b Subzone. On the other hand, the latest Paleocene calcareous nannofossil subzone NP9a is missed, suggesting a minor hiatus at the P/E boundary.

8. Summary and Conclusions

The Santonian-Eocene carbonate succession of Wadi Mizeira, Northeastern Sinai, is subdivided from base to top into the Sudr, the Esna and the Thebes Formations. Eleven nannofossil zones are identified, based on the first and last occurrences (FOs, LOs) of the marker species. The Upper Cretaceous rocks comprise: 1—*Lucianorhabdus cayeuxii* Zone, CC16 (Late Santonian), 2—*Calculites obscurus* Zone, CC17 (Late Santonian-Early Campanian), 3—*Aspidolithus parvus* Zone, CC18 (Early Campanian) and 4—*Micula murus* Zone, CC25c (Late Maastrichtian). The Paleocene rocks comprise, 1—*Chiasmolithus danicus* Zone, NP3 (Late Danian), 2—*Ellipsolithus macellus* Zone, NP4 (Late Danian), 3—*Fasciculithus tympaniformis* Zone, NP5 (Thanethian-Selandian). The Eocene rocks comprise 1—*Discoaster multiradiatus* Zone, NP9b, 2—*Tribrachiatulus contortus* Zone, NP10a, 3—*Discoaster binodosus* Zone, NP11, 4—*Tribrachiatulus orthostylus* Zone, NP 12, and 5—*Discoaster subloadoensis* Zone, NP14 (Ypresian).

Several stratigraphic hiatus were recorded in the studied section. The Cretaceous/Paleogene boundary is marked by the absence of the Late Cretaceous nannofossil Zone; CC26, as well as the Early Paleocene nannofossil biozones, NP1 and NP2 and probably the lower part of NP3. A major hiatus is suggested at the Selandian/Thanethian boundary as indicated by absence of the nannofossil biozones; NP6, NP7 and NP8. On the other hand, the latest Paleocene calcareous nannofossil subzone NP9a is missed, suggesting a minor hiatus at the P/E boundary.

References

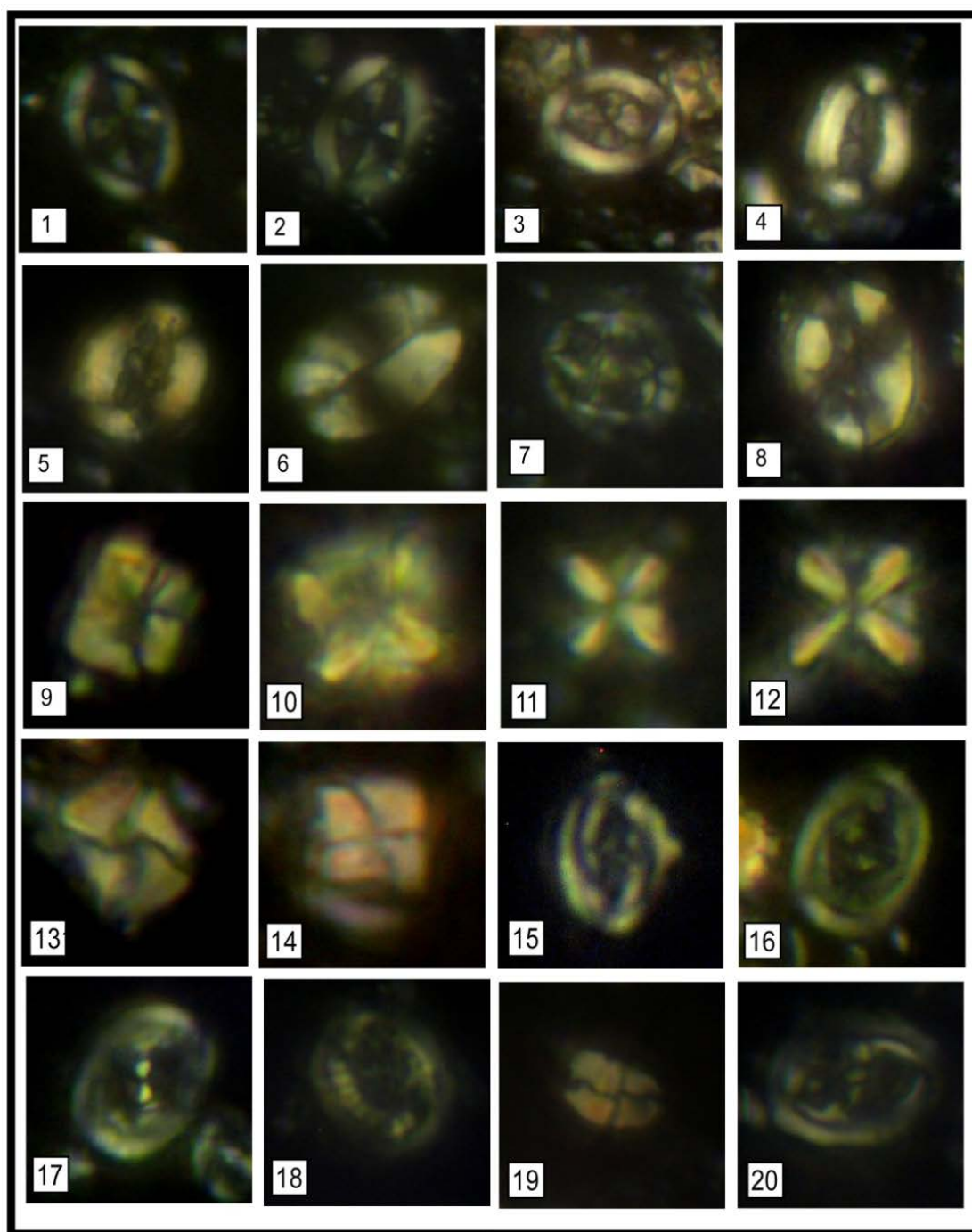
- [1] Moon, F. and Sadek, H. (1923) Preliminary Geological Report on Wadi Gharandal Area (North of Gebel Hammam Faraun, Western Sinai). *Petroleum Research Bulletin*, **12**, 42.
- [2] Moon, F. and Sadek, H. (1925) Preliminary Geological Report on Gabal Khoshera Area Western Sinai. *Petroleum Research Bulletin*, **12**, 42.
- [3] Viotti, C. and El Demerdash, G. (1969) Studies on Eocene Sediments of Wadi Nukhul Area, East Coast-Gulf of Suez. *Proceedings of the 3rd African Micropaleontological Colloquium*, Cairo, 1968, 403-423.
- [4] Youssef, M.I. and Abdelmalik, W.M. (1969) Micropaleontological Zonation of the Tertiary Rocks of Tayiba-Feiran Area, West Central Sinai. *6th Arab. Science Congress*, Damascus, 675-684.
- [5] Abdelmalik, W.M., Bassiouni, M.A. and Obeid, F.L.M.A. (1978) Biostratigraphy of Upper Cretaceous-Lower Tertiary Rocks from West Central Sinai. Part Two: Calcareous nannoplankton. Actes du VIth Colloque African de Micropaleontologie, *Annals des Mines et de la Geologie*, Tunis, 28/2, 217-241.
- [6] El-Boukhary, M. and Abdelmalik, W.A. (1983) Revision of the Stratigraphy of the Eocene Deposits in Egypt (UNESCO project I.G.C.P. No. 183, C.N.R.S., L. A. 319.). *Neues Jahrbuch für Geologie und Paläontologie*, Monatshefte, 321-337.
- [7] El-Heiny, I. and Morsi, S. (1986) Review of the Upper Eocene Deposits in the Gulf of Suez, Egypt. *Egyptian General Petroleum Corporation (EGPC), 8th Exploration Conference*, Cairo, 1986, 18.
- [8] Arafa, A. and El Ashwah, A. (1988) Late Cretaceous Calcareous Nannoplankton Zonation of East El Qusaima Area, Northeast Sinai. *Bulletin of the Faculty of Science, Zagazig University*, **10**, 317-335.
- [9] Arafa, A. (1991) Biostratigraphic Zonation of the Late Cretaceous Sediments of Gabal Nazzazat, South-West Sinai, Egypt. *Annals of the Geological Survey of Egypt*, **17**, 173-182.
- [10] Hewaidy, A., Arafa, A. and El Ashwah, A. (1991) Biostratigraphy of Upper Cretaceous Rocks of El Qusaima Area, North-East Sinai, Egypt. *Annals of the Geological Survey of Egypt*, **17**, 199-212.
- [11] Shahin, A. and Kora, M. (1991) Biostratigraphy of Some Upper Cretaceous Succession in the Eastern Central Sinai, Egypt. *Neues Jahrbuch für Geologie und Paläontologie*, **11**, 671-692.
- [12] Abul-Nasr, R.A. (1992) Paleoecology and Sedimentary Environments of Middle-Upper Eocene Rocks in West Central Sinai, Egypt. *Middle East Research Center, Ain Shams University, Earth Sciences Series*, **6**, 126-138.
- [13] Abul-Nasr, R.A. (1993) Re-Evaluation of the Middle-Upper Eocene Biostratigraphy of West Central Sinai, Egypt. *Middle East Research Center, Ain Shams University, Earth Sciences Series*, **7**, 153-166.
- [14] Abul-Nasr, R.A. and Marzouk, A.M. (1994) Eocene Biostratigraphy of Wadi Wardan, Sinai, with Special Emphasis on Calcareous Nannofossils. *Middle East Research Center, Ain Shams University, Earth Sciences Series*, **8**, 178-187.
- [15] El-Sheikh, H.A. and El-Beshtawy, M.K. (1992) Biostratigraphic Studies on the Late Cretaceous-Early Tertiary between Wnadi Tayiba and Wadi Feiran, West Central Siai, Egypt. *Geology of the Arab World*, Cairo University, Cairo, 395-405.
- [16] Faris, M. (1992) Calcareous Nannoplankton from the Turoniane-Maastrichtian Sequence East of El-Qusaima, North East Sinai, Egypt. *Qatar University Science Journal*, **12**, 166-175, 187-201.
- [17] Faris, M. and Strougo, A. (1992) Biostratigraphy of Calcareous Nannofossils across the Middle Eocene/Upper Eocene Boundary in Egypt. *Middle East Research Center, Ain Shams University, Earth Sciences Series*, **6**, 86-99.
- [18] Lüning, S., Marzouk, A.M., Morsi, A.M. and Kuss, J. (1998) Sequence Stratigraphy of the Upper Cretaceous of Central East Sinai, Egypt. *Cretaceous Research*, **19**, 153-195.
- [19] Lüning, S., Marzouk, A.M. and Kuss, J. (1998) The Paleocene of Central East Sinai, Egypt; "Sequence Stratigraphy" in Monotonous Hemipelagites. *The Journal of Foraminiferal Research*, **28**, 19-39.
- [20] Faris, M., Abd El-Hameed, A.T., Marzouk A.M. and Ghandour, I.M. (1999) Early Paleogene Calcareous Nannofossil and Planktonic Foraminiferal Biostratigraphy in Central Egypt. *Neues Jahrbuch fuer Geologie und Palaeontologie Abhandlungen*, **2132**, 261-288.
- [21] Faris, M., El-Deep, W.Z. and Mandur, M.M. (2000) Biostratigraphy of Some Upper Cretaceous/Lower Eocene Successions in Southwest Sinai, Egypt. *Annals of the Geological Survey of Egypt*, **23**, 135-161.
- [22] Faris, M., Ghandour, I.M. and Maejima, W. (2007) Calcareous Nannofossils Biostratigraphy and Mineralogical Changes across the Cretaceous/Paleogene Boundary at Wadi Nukhul, Southwestern Sinai, Egypt. *Journal of Geosciences, Osaka City University*, **50**, 15-34.
- [23] El-Sheikh, H.A. (1999) Coniacian-Late Campanian Boundaries in Sinai. *Proceedings of the 1st International Conference on Geology of the Arab World*, **2**, 5-20.

- [24] Bauer, J., Marzouk, A.M., Steuber, T. and Kuss, J. (2001) Lithostratigraphy and Biostratigraphy of the Cenomanian-Santonian Strata of Sinai, Egypt. *Cretaceous Research*, **22**, 497-526.
- [25] Bauer, J., Kuss, J. and Steuber, T. (2003) Sequence Architecture and Carbonate Platform Configuration (Late Cenomanian-Santonian), Sinai, Egypt. *Sedimentology*, **50**, 387-414.
<http://dx.doi.org/10.1046/j.1365-3091.2003.00549.x>
- [26] Obaidalla, N.A., and Kassab, A.S. (2002) Integrated Biostratigraphy of the Coniacian-Santonian Sequence, Southwestern Sinai, Egypt. *Egyptian Journal of Paleontology*, **2**, 85-104.
- [27] Faris, M. and Zahran, E. (2002) Calcareous Nannofossil Biostratigraphy of the Late Paleocene/Early Eocene of El-Bruk Area, North Central Sinai, Egypt. *Egyptian Journal of Paleontology*, **2**, 359-369.
- [28] Faris, M. and Abu Shama, A.M. (2003) Calcareous Nannofossil Biostratigraphy of the Upper Cretaceous-Lower Paleocene Succession in the Thamad Area, East Central Sinai, Egypt. *The 3rd International Conference of Geology of Africa*, **1**, 707-732.
- [29] Abu Shama, A. and Faris, M. (2005) Nannofossil Biostratigraphy of the Maastrichtian-Lower Eocene Rocks at Qalit El Gendi Section, Wadi Sudr, West Central Sinai, Egypt. *Egyptian Journal of Paleontology*, **5**, 161-189.
- [30] El-Azabi, M.H. and El-Araby, A. (2007) Depositional Framework and Sequence Stratigraphic Aspects of the Coniacian-Santonian Mixed Siliciclastic/Carbonate Matulla Sediments in Nezzazat and Ekma Blocks, Gulf of Suez, Egypt. *Journal of African Earth Sciences*, **47**, 179-202.
- [31] Samuel, M.D., Ismail, A.A., Akarish, A.I.M. and Zaky, A.H. (2009) Upper Cretaceous Stratigraphy of the Gebel Somar Area, North-Central Sinai, Egypt. *Cretaceous Research*, **30**, 22-34.
- [32] Perch-Nielsen, K. (1985) Mesozoic Calcareous Nannofossils. In: Bolli, H.M., Saunders, J.B. and Perch-Nielsen, K., Eds., *Plankton Stratigraphy*, Cambridge University Press, Cambridge, 329-426.
- [33] Bown, P.R. and Young, J.R. (1998) Techniques. In: Bown, P.R., Ed., *Calcareous Nannofossil Biostratigraphy (British Micropalaeontological Society Publications Series)*, Chapman and Kluwer Academic, London, 16-28.
- [34] Ghorab, M.A. (1961) Abnormal Stratigraphic Features in Ras Gharib Oil Field. *Proceedings of the 3rd Arabian Petroleum Congress*, **2**, 1-10.
- [35] Beadnell, H.J.L. (1905) The Relations of the Eocene and Cretaceous Systems in the Esna-Aswan Reach of the Nile-Valley. *Journal of the Geological Society (London)*, **61**, 667-678.
- [36] Said, R. (1962) The Geology of Egypt. Elsevier Publishing Company, Amsterdam, 377.
- [37] Sissingh, W. (1977) Biostratigraphy of Cretaceous Calcareous Nannoplankton. *Geologie en Mijnbouw*, **56**, 37-65.
- [38] Perch-Nielsen, K. (1981) Les nannofossilscalaires a la limite Cretace-Tertiaire pres de El Kef, Tunisie, Cah. *Cahiers de Micropaleontologie*, **3**, 25-37.
- [39] Burnett, J.A. (1998) Upper Cretaceous. In: Bown, P.R., Ed., *Calcareous Nannofossil Biostratigraphy (British Micropalaeontological Society Publications Series)*, Chapman and Kluwer Academic Publishers, London, 132-199.
- [40] Birkelund, T., Hancock, J.M., Hart, M.B., Rawson, P.E., Remane, J., Robaszynski, F., Schmid, F. and Surlyk, F. (1984) Cretaceous Stage Boundaries Proposals. *Bulletin of the Geological Society of Denmark*, **33**, 3-20.
- [41] Almogi-Labin, A., Eshet, Y., Flexer, A., Honigstein, A., Moshkovitz, S. and Rosenfeld, A. (1991) Detailed Biostratigraphy of the Santonian/Campanian Boundary Interval in Northern Israel. *Journal of Micropaleontology*, **10**, 39-50.
<http://dx.doi.org/10.1144/jm.10.1.39>
- [42] Bralower, T.J. and Siesser, W.G. (1992) Cretaceous Calcareous Nannofossil Biostratigraphy of Sites 761, 762, and 763, Exmouth and Wombat Plateaus, Northwest Australia. *Proceedings of the Ocean Drilling Program, Scientific Results*, **122**, 529-556.
- [43] Isabella, P.S. and Sliter, W.V. (1994) Cretaceous Planktonic Foraminiferal Biostratigraphy and Evolutionary Trends from the Bottaccione Section, Gubbio, Italy. *Palaeontographia*, **82**, 1-89.
- [44] Bralower, T.J. and Mutterlose, J. (1995) Calcareous Nannofossil Biostratigraphy of Site 865, Allison Guyot, Central Pacific Ocean: A Tropical Paleogene Reference Section. *Proceedings of the Ocean Drilling Program, Scientific Results*, **143**, 31-74.
- [45] Gale, A.S., Montgomery, P., Kennedy, W.J., Hancock, J.M., Burnett, J.A. and McArthur, J.M. (1995) Definition and Global Correlation of the Santonian-Campanian Boundary. *Terra Nova*, **7**, 611-622.
- [46] Gale, A.S., Hancock, J.M., Kennedy, W.J., Petrizzo, M.R., Lees, J.A., Walaszczyk, I. and Wray, D.S. (2008) Geochemistry, Stable Oxygen and Carbon Isotopes, Nannofossils, Planktonic Foraminifera, Inoceramid Bivalves, Ammonites and Crinoids of the Waxahachie Dam Spillway Section, North Texas: A Possible Boundary Stratotype for the Base of the Campanian Stage. *Cretaceous Research*, **29**, 131-167.
- [47] Bukry, D. and Bramlette, M.N. (1970) Coccolith Age Determinations, Leg 3, Deep Sea Drilling Project. *Deep Sea*

Drilling Project Initial Reports, **3**, 58-611.

- [48] Perch-Nielsen, K. (1981) New Maastrichtian and Paleocene Calcareous Nannofossils from Africa, Denmark, the USA and the Atlantic, and Some Paleocene Lineages. *Eclogae Geologicae Helvetiae*, **74**, 831-863.
- [49] Cepek, P. and Hay, W.W. (1969) Calcareous Nannoplankton and Biostratigraphic Subdivisions of the Upper Cretaceous. *Gulf Coast Association of Geological Societies Transactions*, **19**, 323-336.
- [50] Romein, A.J.T. (1979) Lineages in Early Paleocene Calcareous Nannoplankton. *Utrecht Micropaleontological Bulletins*, **22**, 18-22.
- [51] Martini, E. (1970) Standard Paleogene Calcareous Nannoplankton Zonation. *Nature*, **1**, 226-560.
- [52] Okada, H. and Bukry, D. (1980) Supplementary Modification and Introduction of Code Numbers to the Low-Latitude Coccolith Biostratigraphic Zonation (Bukry, 1973; 1975). *Marine Micropaleontology*, **5**, 321-325.
[http://dx.doi.org/10.1016/0377-8398\(80\)90016-X](http://dx.doi.org/10.1016/0377-8398(80)90016-X)
- [53] Hay, W.W. and Mohler, H.P. (1967) Calcareous Nannoplankton from Early Tertiary Rocks at Pont Labau, France, and Paleocene-Eocene Correlation. *Journal of Paleontology*, **41**, 1505-1541.
- [54] Perch-Nielsen, K. (1981) Les coccolithes du Paleocene pres de El Kef, Tunisie et leurs ancetres. *Cahiers de Micropaleontologie*, **1981**, 7-23.
- [55] Bramlette, M.N. and Sullivan, F.R. (1961) Coccolithophorids and Related Nannoplankton of the Early Tertiary in California. *Micropaleontology*, **7**, 129-174.
- [56] Martini, E. (1971) Standard Tertiary and Quaternary Calcareous Nannoplankton Zonation. *Proceedings of the 2nd Planktonic Conference*, Roma, 1970, 739-785.
- [57] Gartner Jr., S. (1971) Calcareous Nannofossils from the Joides Blake Plateau Cores and Revision of Paleogene Nannofossil Zonation. *Tulane Studies in Geology and Paleontology*, **8**, 101-121.
- [58] Edwards, A.R. (1971) A Calcareous Nannoplankton Zonation of the New Zealand. Paleogene. *Proceedings of the 2nd Planktonic Conference*, Roma, 1970, 381-419.
- [59] Monechi, S., Bleil, U. and Backman, J. (1985) Magnetobiochronology of Late Cretaceous-Paleogene and Late Cenozoic Pelagic Sedimentary Sequences from the Northwest Pacific (Deep Sea Drilling Project, Leg 86, Site 577). *Proceedings of the Deep Sea Drilling Project, Initial Reports*, **86**, 787-797.
- [60] Müller, C. (1985) Biostratigraphic and Paleoenvironmental Interpretations of the Goban Spur Region Based on a Study of Calcareous Nannoplankton. *Proceedings of the Deep Sea Drilling Project, Initial Reports*, **80**, 573-599.
- [61] Backman, J. (1986) Late Paleocene to Middle Eocene Calcareous Nannofossil Biochronology from the Shatsky Rise, Walvis Ridge and Italy. *Palaeogeography, Palaeoclimatology, Palaeoecology*, **57**, 43-59.
[http://dx.doi.org/10.1016/0031-0182\(86\)90005-2](http://dx.doi.org/10.1016/0031-0182(86)90005-2)
- [62] Berggren, W.A., Kent, D.V., Swisher, C.C. and Aubry, M.P. (1995) A Revised Cenozoic Geochronology and Chronostratigraphy. Society for Sedimentary Geology (SEPM), Special Publication, Tulsa, 129-212.
- [63] Berggren, W.A., Aubry, M.P., van Fossen, M., Kent, D.V., Norris, R.D. and Quillévéré, F. (2000) Integrated Paleocene Calcareous Plankton Magnetobiochronology and Stable Isotope Stratigraphy: DSDP Site 384 (NW Atlantic Ocean). *Palaeogeography, Palaeoclimatology, Palaeoecology*, **159**, 1-51.
- [64] Raffi, I., Backman, J. and Pälike, H. (2005) Changes in Calcareous Nannofossil Assemblage across the Paleocene/Eocene Transition from the Paleo-Equatorial Pacific Ocean. *Palaeogeography, Palaeoclimatology, Palaeoecology*, **226**, 93-126. <http://dx.doi.org/10.1016/j.palaeo.2005.05.006>
- [65] Agnini, C., Fornaciari, E., Rio, D., Tateo, F., Backman, J. and Giusberti, L. (2007) Responses of Calcareous Nannofossil Assemblages, Mineralogy and Geochemistry to the Environmental Perturbations across the Paleocene/Eocene Boundary in the Venetian Pre-Alps. *Marine Micropaleontology*, **63**, 19-38.
- [66] Hay, W.W. (1964) The Use of the Electron Microscope in the Study of Fossils. *Smithsonian Institution Annual Reports*, **163**, 409-415.
- [67] Bukry, D. (1973) Low-Latitude Coccolithbiostratigraphic Zonation. *Proceedings of the Deep Sea Drilling Project, Initial Reports*, **15**, 685-703.
- [68] Hekel, H. (1968) Nannoplanktonhorizonte und tektonische strukturen in der flyschzonenordlich von Wien (Bisambergzuge). *Jahrbuch der Geologischen Bundesanstalt*, **3**, 293-337.
- [69] Aubry, M.P. (1996) Towards an Upper Paleocene-Lower Eocene High Resolution Stratigraphy Based on Calcareous Nannofossil Stratigraphy. *Israel Journal of Earth Sciences*, **44**, 239-253.
- [70] Faris, M. and Strougo, A. (1998) The Lower Libyan in Farafra (Western Desert) and Luxor (Nile Valley): Correlation by Calcareous Nannofossils. *Middle East Research Center, Ain Shams University, Earth Sciences Series*, **12**, 137-156.
- [71] Aubry, M.P., Berggren, W.A., Cranner, B., Dupius, D.V., Ouda, K., Schmitz, B. and Steurbaut, E. (1999) Paleo-

- cene/Eocene Boundaries Sections in Egypt. In: Ouda, K. and Soliman, H., Eds., *Late Paleocene-Early Eocene Events from Northern Africa to the Middle East. International Symposium in Connection with First International Conference on the Geology of Africa*, Assiut, 1-11.
- [72] Strougo, A. and Faris, M. (1993) Paleocene-Eocene Stratigraphy of Wadi El Dakhla, Southern Galala Plateau. Ain Shams University, Middle East Research Centre Publisher, Marsá Maṭrūḥ, 49-62.
 - [73] Bronnimann, P. and Stadner, H. (1960) Die Foraminiferen- und Discoasteridenzonen von Kuba und ihre interkontinentale correlation. *Erdöl-Zeitschrift*, **76**, 364-369.
 - [74] Faris, M. (1991) Late Cretaceous Calcareous Nannofossils and Stage Boundaries in East Mubarak, Well No. 1, Western Desert, Egypt. *Annals of the Geological Survey of Egypt*, **17**, 213-221.
 - [75] Ayyad, S.N., Faris, M., El Nahass, H.A. and Saad, K.A.A. (2003) Planktonic Foraminifera and Calcareous Nannofossil Biostratigraphy from the Upper Cretaceous-Lower Eocene Successions in Northeast Sinai, Egypt. *The 3th International Conference on the Geology of Africa*, Assiut, 7-9 December 2003, 649-683.
 - [76] Faris, M. and Farouk, S. (2012) Integrated Biostratigraphy of Two Upper Maastrichtian–Palaeocene Successions in North-Central Sinai, Egypt. *Geologia Croatica*, **65**, 139-160.
 - [77] El-Deeb, M., Faris, M. and Mandour, M. (2000) Upper Cretaceous-Lower Paleogene Foraminiferal Paleocology of North and Southwest Sinai Areas, Egypt. *Egyptian Journal of Petroleum*, **9**, 105-122.
 - [78] Faris, M. and Salem, R.F. (2007) Paleocene-Early Eocene Calcareous Nannofossil Biostratigraphy in West Central Sinai, Egypt. *Proceeding of the 8th Conference Geology of Sinai for Development*, Ismailia, 1-14.
 - [79] Farouk, S. and Faris, M. (2008) Campanian to Eocene Planktic Foraminiferal and Calcareous Nannofossil Biostratigraphy in the Synclinal Areas around Gebel Libni, North Sinai, Egypt. Ain Shams University, Middle East Research Centre Publisher, Marsá Maṭrūḥ, 187-201.
 - [80] Farouk, S. and Faris, M. (2012) Late Cretaceous Calcareous Nannofossil and Planktonic Foraminiferal Bioevents of the Shallow-Marine Carbonate Platform in the Mitla Pass, West Central Sinai, and Egypt. *Cretaceous Research*, **33**, 50-65. <http://dx.doi.org/10.1016/j.cretres.2011.08.002>



10 um

Plate 1. All figures $\times 1250$. 1-3. *Arkhangelskiella cymbiformis* Vekshina, 1—sample no. 1, 2—sample no. 28, 3—sample no. 38. 4, 5. *Aspidolithus parvus* (Stradner), 4—sample no. 46, 5—sample no. 53. 6. *Prolatipatella multicarinata* (Gartner), sample no. 26. 7. *Prediscosphaera cretacea* (Arkhangelsky), sample no. 25. 8. *Eiffellithus tur-riseiffelii* (Deflandre in Deflandre & Fert), sample no. 24. 9, 13, 14. *Micula murus* (Martini), 9—sample no. 51, 13—sample no. 54, 14—sample no. 57. 10-12. *Micula decussata* Vekshina, 10—sample no. 8, 11—sample no. 13, 12—sample no. 22. 15, 20. *Placozygus sigmoides* (Bramlette & Sullivan), 15—sample no. 65, 20—sample no. 71. 16, 17. *Reinhardtites anthophorus* (Deflandre), 16—sample no. 6, 17—sample no. 14. 18. *Cribrosphaerella ehrenbergii* (Arkhangelsky), sample no. 2. 19. *Calculites obscures* (Deflandre), sample no. 15.

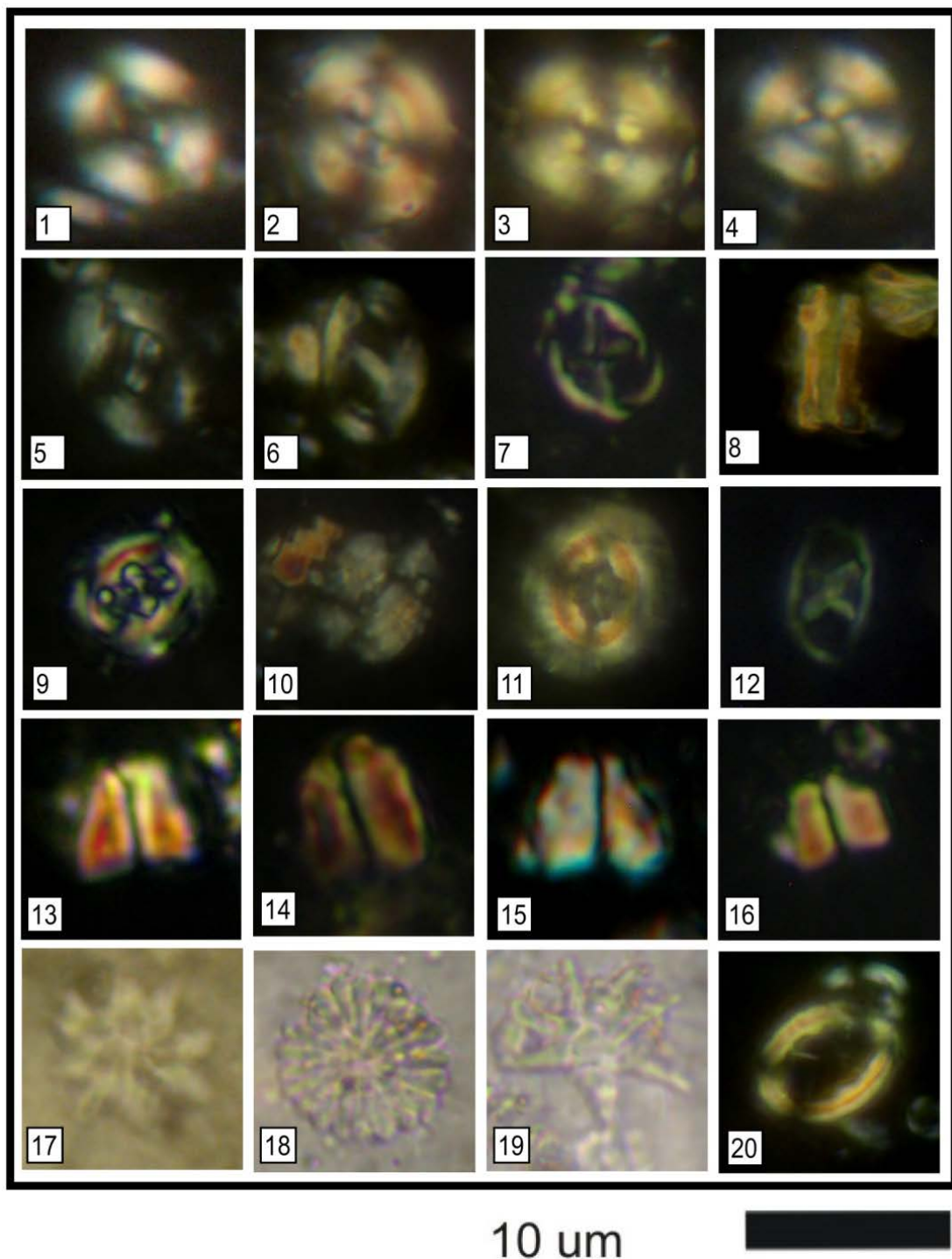


Plate 2. All figures $\times 1250$. 1-3, 4. *Watznaueria barnesae* (Black in Black & Barnes), 1—sample no. 11, 2—sample no. 36, 3—sample no. 39, 4—sample no. 40. 5-6. *Zygodiscus plectopons* (Bramlette & Sullivan), 5—sample no. 75, 6—sample no. 80. 7. *Neococcolithes protenus* (Bramlette & Sullivan), sample no. 92. 8. *Lucianorhabdus cayeuxii* Deflandre, sample no. 29. 9. *Chiasmolithus danicus* (Brotzen), sample no. 76. 10. *Ellipsolithus macellus* (Bramlette & Sullivan), sample no. 94. 11. *Ericsonia formosa* (Kamptner), sample no. 113. 12. *Neococcolithes dubius* (Deflandre), sample no. 114. 13, 15. *Fasciculithus clinatus* Bukry, 13—sample no. 83, 15—sample no. 85. 14-16. *Fasciculithus tympaniformis* (Hay & Mohler), 14—sample no. 78, 16—sample no. 81. 17. *Discoaster barbadiensis* Tan, sample no. 87. 18. *Discoaster multiradiatus* Bramlette & Reidel, sample no. 86. 19. *Discoaster araneus* Bukry, sample no. 88. 20. *Chiasmolithus solitus* (Bramlette & Sullivan), sample no. 118.

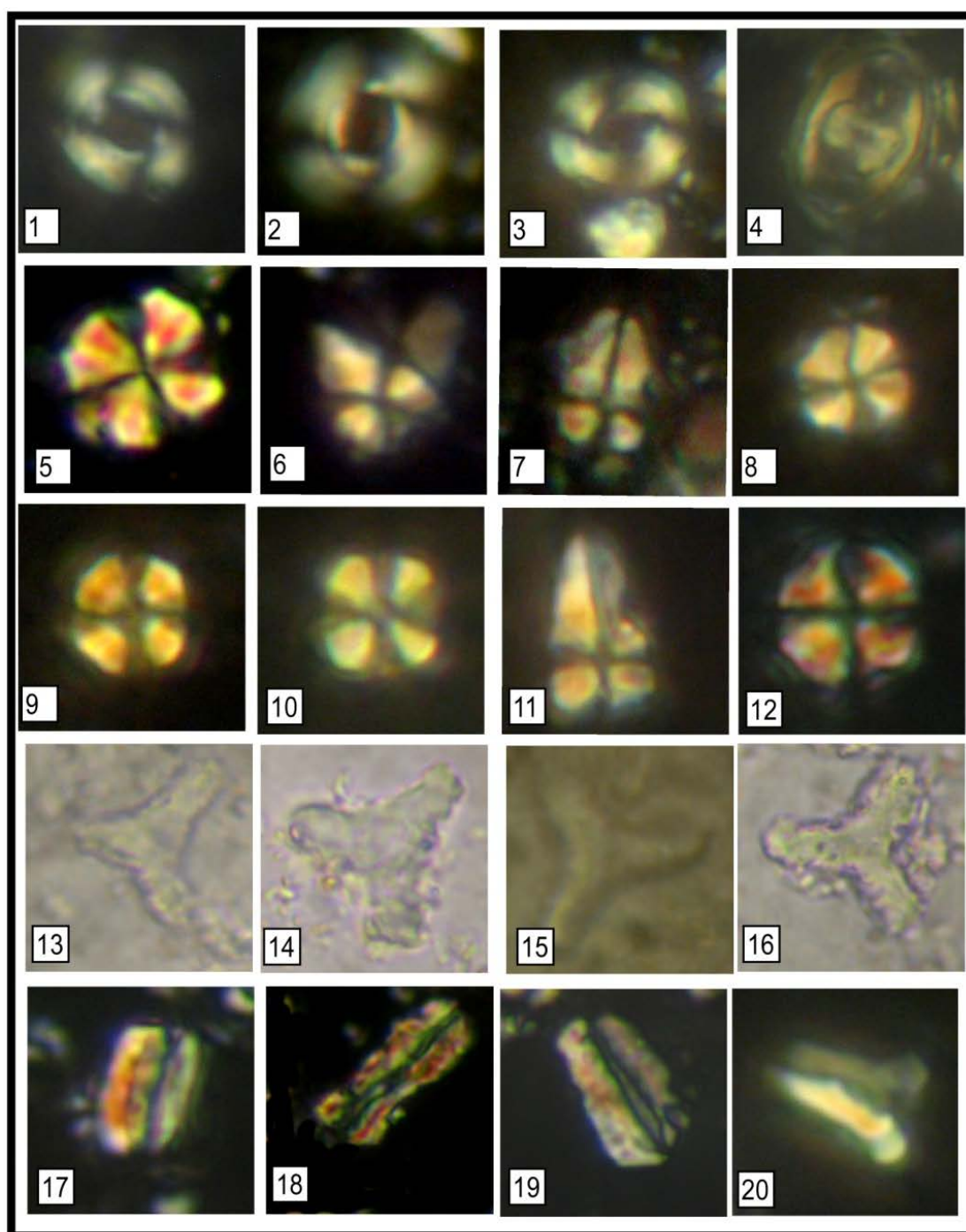
10 μm

Plate 3. All figures $\times 1250$. 1, 3. *Reticulofenestra dictyoda* (Deflandre), 1—sample no. 109, 3—sample no. 113. 2. *Reticulofenestra umbilica* (Levin), sample no. 102, 4—*Zeugrhabdotus pseudanthophorus* (Bramlette & Martini), sample no. 46. 5, 8, 9, 10, 12. *Sphenolithus moriformis* (Bronnimann & Stradner), 5—sample no. 91, 8—sample no. 101, 9—sample no. 105, 10—sample no. 106, 12—sample no. 113. 6. *Sphenolithus obtusus* Bukry, sample no. 118. 7, 11. *Sphenolithus radians* Deflandre, 7—sample no. 97, 11—sample no. 99. 13-16. *Tribrachiatus orthostylus* Shamrai, 13—sample no. 102, 14—sample no. 105, 15—sample no. 106, 16—sample no. 108. 17-20. *Zygrhablithus bijugatus* (Deflandre), 17—sample no. 87, 18—sample no. 90, 19—sample no. 93.